Effect of Minoxidil on Trabecular Outflow via the Paracellular Pathway

Hyun Gu Kang[1], Jae Woo Kim[2]

[1]Cheil Eye Hospital, Daegu, Korea
[2]Department of Ophthalmology, Daegu Catholic University School of Medicine, Daegu, Korea

Purpose: To investigate the pathway and effects of minoxidil on trabecular outflow in cultured human trabecular meshwork (TM) cells.

Methods: After exposing primarily cultured TM cells to 0, 10, 50, or 100 μM minoxidil sulfate (MS), trabecular outflow was assessed by measuring TM cell monolayer permeability to carboxyfluorescein and transepithelial electrical resistance. To assess the pathway of permeability changes, caveolin-1, occludin, and claudin-5 levels were measured via western blot. Generation of reactive oxygen species (ROS) was measured using the dichlorofluorescein diacetate assay. To assess the involvement of nitric oxide (NO) in minoxidil-induced permeability increase, the degrees of endothelial nitric oxide synthase mRNA expression and NO production were measured with reverse transcription polymerase chain reaction and Griess assays, respectively. Permeability was also measured with co-exposure to 50 μM N-acetyl cysteine.

Results: MS significantly increased TM cell monolayer permeability ($p < 0.05$) and decreased transepithelial electrical resistance ($p < 0.05$). MS decreased the degree of endothelial nitric oxide synthase mRNA expression but did not affect NO production. MS decreased occludin and claudin-5 levels but did not affect caveolin-1 level. MS at 100 μM increased the generation of ROS, and MS-induced permeability increase was attenuated after co-exposure to 50 μM N-acetyl cysteine.

Conclusions: Minoxidil may preferentially increase trabecular permeability via a paracellular pathway by downregulation of tight junction proteins. This minoxidil-induced permeability through the TM may be mediated by generation of ROS.

Key Words: Minoxidil, Permeability, Reactive oxygen species, Trabecular meshwork

The trabecular meshwork (TM) is involved in regulation of aqueous humor outflow to control intraocular pressure (IOP). It is thought that impaired drainage through the tra-becular pathway caused by increased resistance is the primary cause of increased IOP in primary open-angle glaucoma [1,2]. While most glaucoma medications approved for clinical use act either on the uveoscleral pathway and/or aqueous humor formation, several new drugs targeting the trabecular outflow pathway have recently entered clinical development [3].

K_{ATP} channel openers are a structurally diverse group of drugs with a broad spectrum of potential therapeutic ap-

plications. Among them, minoxidil is used topically to stimulate hair growth [4]. Minoxidil is also a direct vasodilator introduced for treatment of hypertension as it is capable of reducing blood pressure in patients with resistant hypertension in whom therapy has failed with other multidrug regimens [5]. Although minoxidil induced ocular hypotension when given topically in an animal study [6], further studies focusing on IOP-lowering activity have not been reported. However, previous studies revealed that minoxidil induced an increase in blood-brain tumor barrier permeability [7-9].

Transport of plasma proteins and solutes across the endothelium involves two different routes. The first is transcellular via caveolae-mediated vesicular transport, and the second is paracellular through inter-endothelial junctions [10]. Paracellular permeability of the endothelial barrier is maintained by inter-endothelial junctions that are regulated by expression of claudin-5 and occludin. In contrast, transcellular transport occurs via fission of plasma membrane macrodomains enriched with caveolin-1 (CAV-1) and caveolae from the luminal surface of the endothelium, followed by transport of caveolar vesicles to the basal surface. Caveolae and CAV-1 mediate endocytosis and transcytosis in endothelial cells [11-13]. In the eye, CAV-1 is expressed in TM cells, and dysregulation of the expression of caveolin in the TM has been implicated in the pathology of primary open angle glaucoma [14].

Minoxidil induces accelerated formation of transport vesicles in both the brain tumor capillary endothelium and tumor cells [7,15] suggesting that vesicular transport is largely responsible for the enhanced permeability induced by minoxidil rather than the opening of endothelial tight junctions (TJ). On the contrary, another study demonstrated that minoxidil also involves the paracellular pathway by downregulating the expression of occludin and claudin-5 [16]. Previous studies have shown that minoxidil-induced permeability may be related to accelerated formation of CAV-1 protein and could be mediated by reactive oxygen species (ROS). Minoxidil also improves paracellular transport by regulating the expression of TJ proteins, possibly mediated by ROS [8,9,15].

TM cells regulate trabecular outflow because they have endothelial cell-like and muscle cell-like properties [17-21]. As minoxidil acts as a vasodilator and increases permeability, it is possible that minoxidil increases trabecular outflow; however, the effect and mechanism of minoxidil-induced permeability increase have not yet been studied in

the TM. This study was performed to determine whether minoxidil affects the permeability of TM. In addition, we studied the mechanism of minoxidil-induced permeability changes and whether this process was regulated by ROS.

Materials and Methods

Cell culture and treatment

This study followed the tenets of the Declaration of Helsinki and was approved by the institutional review board/ethics committee of Daegu Catholic University Hospital (CR-18-106-L). TM cell cultures were established from enucleated human eyes obtained from an eye bank. Briefly, TM tissues were excised by dissecting a continuous strand of tissue between the line of Schwalbe and the scleral spur. The excised TM tissues were placed in a sterile culture dish and left undisturbed at 37°C in a 5% CO_2 atmosphere. After noting initial cell growth, the explants were removed, and the cultures were maintained with a medium containing 10% fetal bovine serum. Primarily cultured TM cells were then exposed to 0, 10, 50, or 100 µM minoxidil sulfate (MS; Sigma, St. Louis, MO, USA). In addition, TM cells were co-exposed to 50 µM N-acetyl cysteine (NAC, Sigma) to evaluate the effect of ROS on MS-induced permeability changes.

MTT assay for cell viability

Cell survival was determined using a rapid 3-(4, 5–dimethylthiazol-2-yl)-2, 5-diphenyltetrazolium bromide (MTT, Sigma) colorimetric assay [22,23]. For the assay, 100 µL of a MTT stock solution (5 mg MTT/mL PBS) was added to each well and incubated for 4 hours at 37°C, after which all media was removed from the well. After 0.5 mL of dimethyl sulfoxide (Sigma) was added to each well, 100 µL of solution from each well was transferred to a 96-well plate and analyzed using a multi-well scanning spectrophotometer (λ = 570 nm).

Measurement of monolayer cell permeability with carboxyfluorescein

Permeability of the TM cell monolayer was measured using carboxyfluorescein as previously described with mi-

nor modification [24-27]. Briefly, primary cultured human TM cells were incubated in the inner chamber (insert diameter, 12 mm; pore size, 0.4 μm) of a 12-well plate (no. 3460, Transwell; Corning, Lowell, MA, USA) supplemented with 10% fetal bovine serum. After the cells reached confluence, the media was changed to 1% serum containing DMEM to avoid the effects of growth factors and proteins. Then, the TM cells were exposed to each drug for 24 hours. After washing, 50 μM of the tracer carboxyfluorescein (Sigma-Aldrich, St. Louis, MO, USA) was added to each well. The media was collected from the outer well to analyze fluorescence after 2 hours, and the concentration of carboxyfluorescein in the collected media was measured using a spectrofluorometer (FLUOstar Optima; BMG Labtech, Offenburg, Germany) with an excitation wavelength of 490 nm and an emission wavelength of 530 nm.

Measurement of monolayer transepithelial electrical resistance

TM cells were seeded at 2×10^4 cells/well and grown until confluent in the inner well (pore size, 0.4 μm; diameter, 12 mm) of 12-well culture plates (Transwell, Corning) [28,29]. Four hours after each drug exposure, transepithelial electrical resistance (TEER) was measured with an electrical resistance system (epithelial voltohmmeter, EVOM2; World Precision Instruments, Sarasota, FL, USA) according to the manufacturer's instructions. The results were recorded and expressed as net value ($\Omega \, cm^2$).

Griess assay for nitric oxide production and reverse transcription polymerase chain reaction for endothelial nitric oxide synthase mRNA expression

To evaluate the effect of MS on production of nitric oxide (NO), nitrite concentrations in the media were measured using the Griess reaction [30]. Briefly, media samples were collected from each well following appropriate treatment and reacted with modified Griess reagent (Sigma-Aldrich) by mixing equal volumes at room temperature for 15 minutes. Optical density was then measured and recorded on a multi-well scanning spectrophotometer at 540 nm. To evaluate the effect of MS on expression of endothelial nitric oxide synthase (eNOS) mRNA, reverse transcription polymerase chain reaction (RT-PCR) was performed as follows. After exposure to MS, total RNA was extracted using Trizol reagent (Invitrogen, Carlsbad, CA, USA). An RNA denaturation mix consisting of isolated RNA, oligo dT primers, and nuclease-free water was denatured. RT-PCR was performed using oligonucleotide primers specific to eNOS. cDNA was synthesized by adding prime RT premix, Taq Green Master Mix, and 10 pM of each forward and reverse primer (forward primer, 5' CTG GCT TTC CCT TCC AGT TC 3', 225 bp; reverse primer, 5' CCT TCC AGA TTA AGG CGG AC 3', 225 bp) were added to the synthesized cDNA. The amplification reaction was carried out for 30 cycles on a DNA Engine Cycler (Bio-Rad, Hercules, CA, USA). The amplified PCR products were analyzed using Multi-gauge software (Fujifilm, Tokyo, Japan) after electrophoresis. β-actin was used as an internal standard.

Measurement of CAV-1, occludin, and claudin-5 levels by western blotting

Cell extracts were prepared by lysing cells with RIPA buffer (Thermo Scientific, Carlsbad, CA, USA). Samples were sonicated and cleared by centrifugation (1,200 rpm) at 4°C for 10 minutes. Supernatant protein concentrations were determined using BCA protein assays (Thermo Scientific, Carlsbad, CA, USA). Samples containing equal amounts of protein were separated by NuPAGE 4-12% Bis-Tris gels (Invitrogen), followed by transfer of resolved proteins to nitrocellulose membranes using the XCell Sure-Lock electrophoresis system (Invitrogen). Nonspecific binding was blocked for 1 hour at room temperature. Blots were then probed overnight at 4°C with primary antibodies, followed by 1-hour incubation with secondary antibodies conjugated to goat anti-rabbit horseradish peroxidase (Santa Cruz Biotechnology, Dallas, TX, USA). Western blots were developed using Super Signal West Pico Chemiluminescent substrate (Thermo Scientific). Quantification of the signals was performed using the Gel Doc XR+ system (Bio-Rad). Glyceraldehyde 3-phosphate dehydrogenase was used as an internal standard.

Measurement of ROS production by dichlorofluorescein diacetate assay

Generation of ROS was measured using the dichlorofluorescein diacetate assay [31,32]. After treatment of cells in a 96-well culture plate, the medium was removed, and

cells were subsequently washed. Cells were then treated with 5 µM dichlorofluorescein diacetate (Sigma), after which they were incubated for 30 minutes at 37°C in the dark. The change in fluorescence of oxidized dichlorofluorescein was measured at excitation and emission wavelengths of 488 nm and 527 nm, respectively, using a fluorescence analyzer (FLUOstar OPTIMA).

Statistical analysis

All data represent the average results of at least three independent experiments. Experimental differences between the results of control cultures and a single treatment group were evaluated using Student's t-test. A p-value less than 0.05 was considered statistically significant.

Results

Cell culture

The TM cells grew into the surrounding tissue explants as a monolayer after 2 weeks of primary culture. The presence of TM cells was confirmed by their characteristic morphology and characteristic growth pattern as satellite colonies distant from the tissue explants [33].

Effect of MS on the viability of TM cells

Exposure to 0, 10, 50, or 100 µM MS for 24 hours did not significantly affect TM cell survival (all $p > 0.05$) (Fig. 1).

Effects of MS on TM cell monolayer permeability

TEER represents the resistance to flow through the TM cell monolayer. Exposure to 10, 50, or 100 µM MS significantly decreased TEER of the TM cell monolayer ($p = 0.007$, 0.033, 0.004, respectively) (Fig. 2A). In addition, exposure to 10 µM MS significantly decreased TEER after 2, 3, and 4 hours ($p = 0.018$, 0.033, 0.013, respectively) (Fig. 2B). To evaluate the effect of MS on permeability through the paracellular pathway, monolayer cell permeability was measured using carboxyfluorescein [10]. As a result, exposure to 10, 50, or 100 µM MS significantly increased the concentration of carboxyfluorescein in the outer well compared to non-exposed controls ($p = 0.037$, 0.038, 0.014, respectively) (Fig. 3).
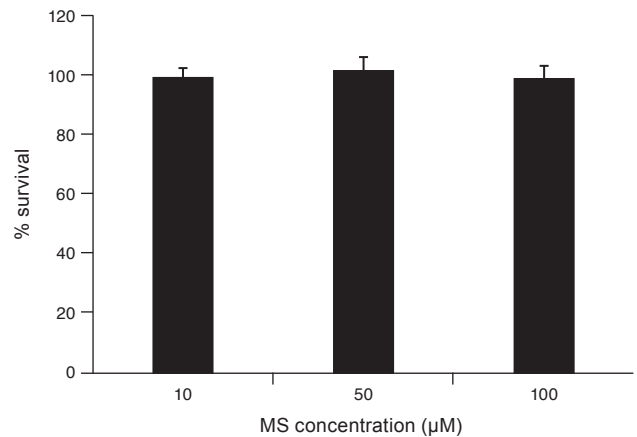

Fig. 1. Effect of minoxidil sulfate (MS) on the survival of cultured human trabecular meshwork cells. MS did not affect the survival of trabecular meshwork cells compared to non-exposed controls (all $p > 0.05$).
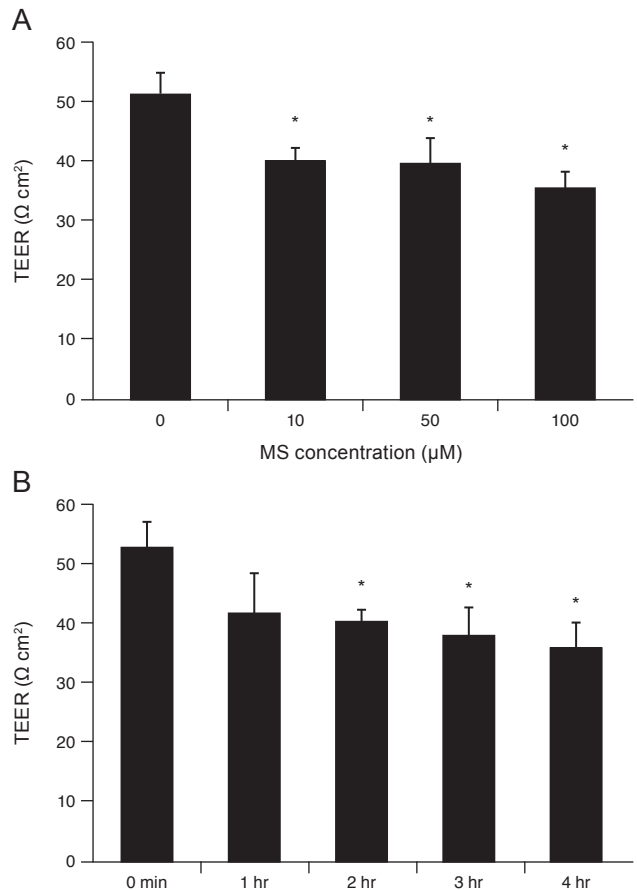

Fig. 2. Effect of minoxidil sulfate (MS) on the transepithelial electrical resistance (TEER) of the trabecular meshwork cell monolayer. (A) Exposure to 10, 50, or 100 µM MS significantly decreased TEER compared with non-exposed controls (*$p < 0.05$). (B) Exposure to 10 µM MS significantly decreased TEER in a time-dependent manner (*$p < 0.05$).

Effects of MS on NO production and eNOS mRNA expression

Exposure to 0, 10, 50, or 100 μM MS did not significantly affect nitrite concentration in the media compared to non-exposed controls (all $p > 0.05$) (Fig. 4). Exposure to 50 μM and 100 μM MS significantly decreased eNOS mRNA expression ($p = 0.004$ and 0.019, respectively) (Fig. 5).

Effects of MS on CAV-1, occludin, and claudin-5 levels

Exposure to 0, 10, 50, or 100 μM MS did not affect CAV-1 level compared to non-exposed controls (all $p > 0.05$)
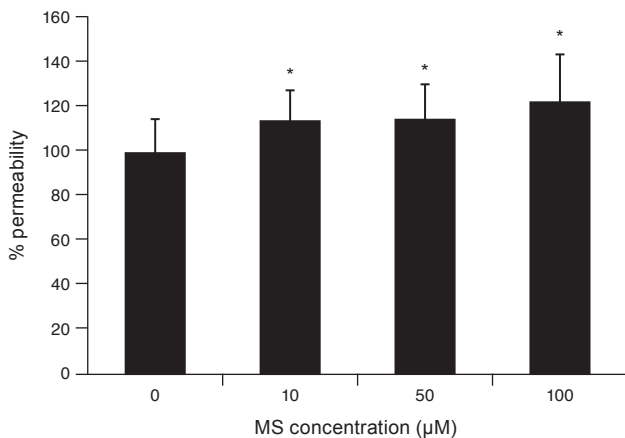
(Fig. 6), suggesting that MS-induced permeability increase is not associated with the transcellular pathway. In contrast, exposure to 10, 50, or 100 μM MS significantly decreased occludin level ($p = 0.045$, 0.002, 0.002, respectively) (Fig. 7). Furthermore, exposure to 50 or 100 μM MS significantly decreased claudin-5 level ($p = 0.037$, 0.001, respectively) (Fig. 8). Taken together, these results revealed that MS increased trabecular permeability through the paracellular pathway.

Fig. 3. Effect of minoxidil sulfate (MS) on trabecular meshwork cell monolayer permeability. Exposure to 10, 50, or 100 μM MS significantly increased permeability of the trabecular meshwork ($^*p < 0.05$). Carboxyfluorescein intensity of the outer chamber was normalized to the mean value obtained with a non-exposed control (permeability 100%).
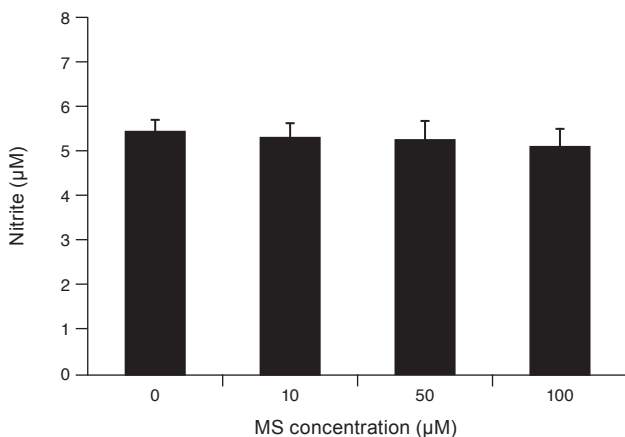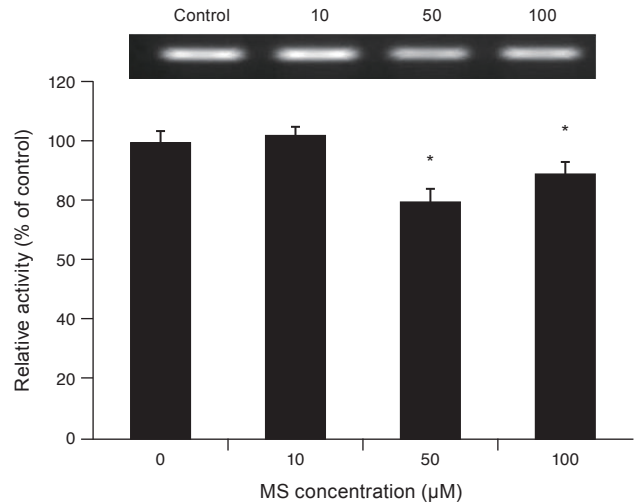

Fig. 5. Effect of minoxidil sulfate (MS) on the expression of endothelial nitric oxide synthase mRNA measured with reverse transcription polymerase chain reaction in trabecular meshwork cells. Exposure to 50 or 100 μM MS significantly decreased the expression of endothelial nitric oxide synthase mRNA compared to non-exposed controls ($^*p < 0.05$).

Fig. 4. Effect of minoxidil sulfate (MS) on the production of nitric oxide. Exposure to MS did not affect the production of nitric oxide compared to non-exposed controls (all $p > 0.05$).
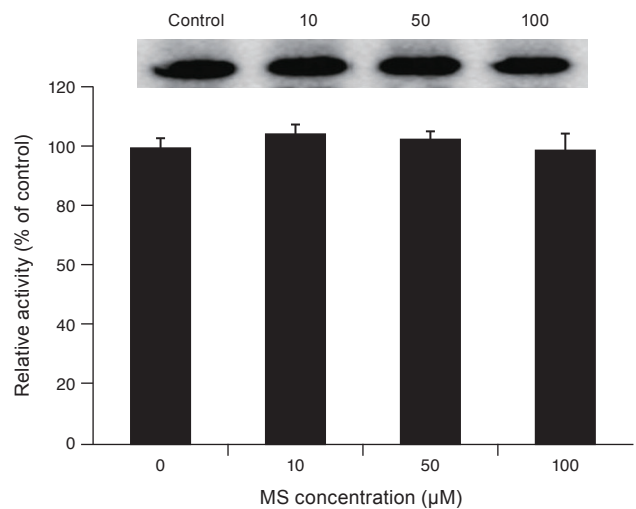

Fig. 6. Effect of minoxidil sulfate (MS) on the level of caveolin-1 protein measured with western blot. Exposure to MS did not affect caveolin-1 level compared to non-exposed controls (all $p > 0.05$).

Effects of MS on ROS generation

Exposure to 100 µM MS significantly increased ROS generation after 1 and 2 hours exposure ($p = 0.002$, 0.001, respectively) (Fig. 9). Co-exposure to the antioxidant NAC (50 µM) significantly attenuated MS-induced permeability increase compared to exposure to 10, 50, or 100 µM minoxidil alone (*; $p = 0.010$, 0.009, 0.032, respectively) (Fig. 10).

Discussion

While the paracellular route restricts passage of solutes larger than 3 nm in radius, transcellular vesicle trafficking selectively transports macromolecules across the endothelium [10]. Transcellular and paracellular pathways have generally been considered independent processes regulating endothelial barrier function. However, growing evi-
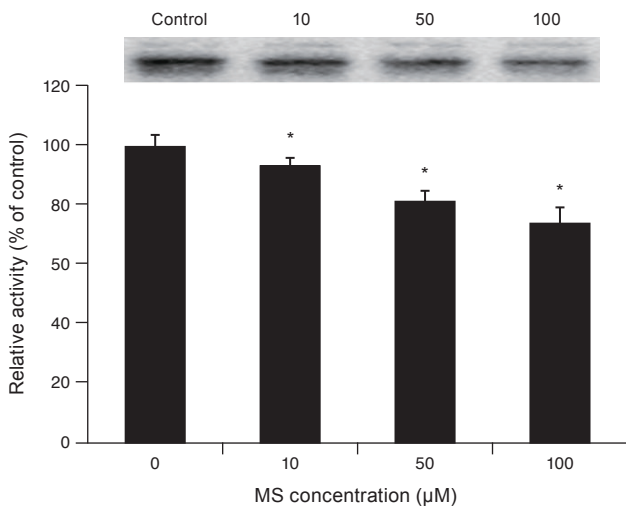

Fig. 7. Effect of minoxidil sulfate (MS) on the level of occludin protein measured with western blot. Exposure to 10, 50, or 100 µM MS significantly decreased occludin level (*$p < 0.05$).
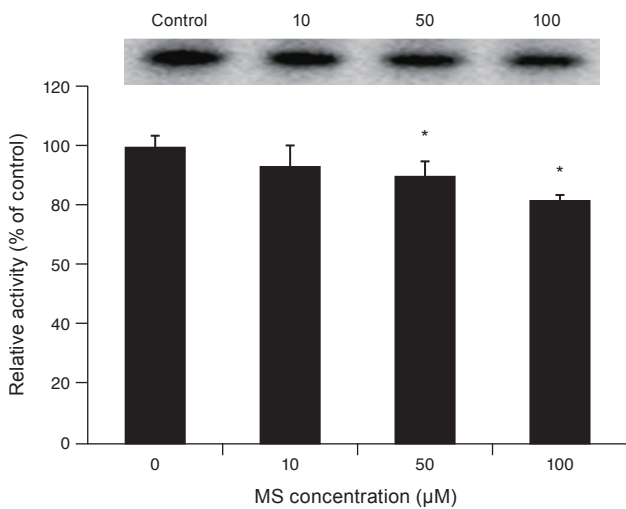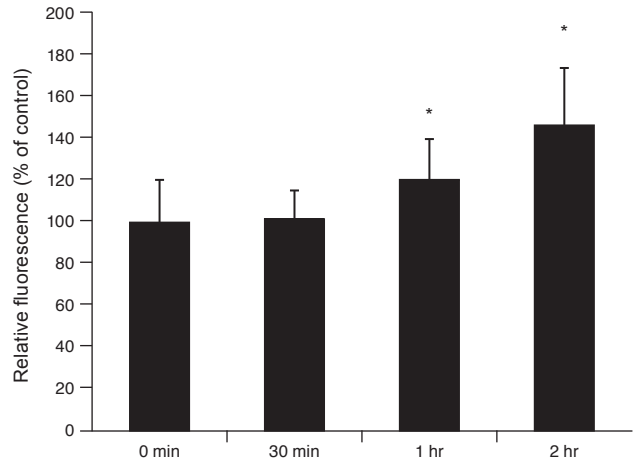

Fig. 8. Effect of minoxidil sulfate (MS) on the level of claudin-5 protein measured with western blot. Exposure to 50 or 100 µM MS significantly decreased claudin-5 level (*$p < 0.05$).

Fig. 9. Effect of minoxidil sulfate on generation of reactive oxygen species measured using the dichlorofluorescein diacetate assay. Exposure to 100 µM minoxidil sulfate significantly increased generation of reactive oxygen species after 1 and 2 hours of exposure (*$p < 0.05$).
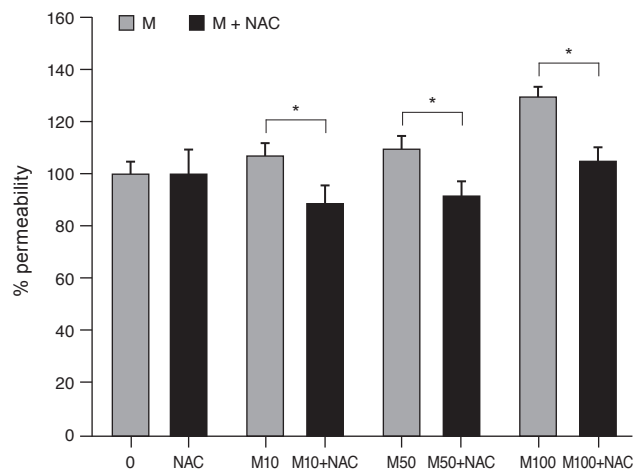
Fig. 10. Effect of antioxidant on the minoxidil (M) sulfate-induced permeability increase measured using the carboxyfluorescein assay. Co-exposure to 50 µM N-acetyl cysteine (NAC) significantly decreased permeability compared to exposure to M sulfate alone at each concentration (µM) (*$p < 0.05$). Carboxyfluorescein intensity of the outer chamber was normalized to the mean value obtained using a non-exposed control (permeability 100%).

dence favors the concept of interdependence between the paracellular and transcellular pathways for maintenance of tissue fluid homeostasis [10,34].

Minoxidil is used as an anti-hypertensive drug as it is known to increase blood-brain barrier permeability [6,9,17]. MS not only increases transcellular permeability by increasing CAV-1 activity, but also increases the paracellular pathway by decreasing occludin and claudin-5 activity [7,15,16].

In the present study, we demonstrated that MS increases trabecular permeability because it decreased TEER. To clarify the route of this permeability increase, we measured the levels of proteins involved in regulation of each route. We found that MS had no significant effect on the protein expression level of CAV-1, which regulates the transcellular pathway. However, MS significantly increased levels of the TJ proteins occludin and claudin-5, which regulate the paracellular pathway. These results indicate that MS increases trabecular outflow through the paracellular route rather than the transcellular route. This enhanced paracellular transport by MS is further supported by the finding that MS increased the permeability of carboxyfluorescein, which is transported via the paracellular pathway.

Outflow through the TM occurs via both transcellular and paracellular pathways [35-37]. It is well known that intercellular transport accounts for only a small fraction of the aqueous humor that leaves the eye by the conventional route, and aqueous humor outflow occurs via the transcellular route through minute pores and giant vacuoles [38-40]. Although MS increased paracellular transport in this study, the effect of MS on the transcellular pathway cannot be excluded because there is a difference between in vitro and physiological conditions, and the two pathways are closely linked and regulated [10]. Due to the complexity of TM outflow and the general limitation of in vitro experiments in the field, in vivo studies should be further investigated.

One previous study using a rabbit model reported that topical MS treatment decreased IOP and suggested that this MS-induced IOP-lowering effect might be mediated by NO [6]. In addition, MS was found to increase CAV-1 level, which has been shown to act as a negative regulator of eNOS [41-44]. To evaluate whether the MS-induced permeability increase was mediated via NO in the TM, we measured NO production and eNOS mRNA expression after MS treatment. The effect of NO on the MS-induced perme-

ability increase was not significant as MS did not affect generation of NO. On the other hand, MS at high concentrations decreased eNOS mRNA expression. This decreased eNOS mRNA expression may result from the increased activity of CAV-1, though no such observation was noted in our study. This might seem paradoxical in view of the postulated role of caveolae in negative regulation of eNOS; however, Yu et al. [45] elegantly demonstrated that eNOS activation is lost in the absence of CAV1 and caveolae and proposed that eNOS activation might require caveolae. Until now, multiple roles of caveolae are still under investigation and need further study, especially in the TM [46].

Another possible explanation is that the activity of increased CAV-1 expression may precede the decreased expression of occludin and claudin-5 [10,16]. These previous studies demonstrated that an increase in endothelial CAV-1 expression change occurs early, while alterations of the TJ proteins occludin and claudin occur later in the time course. Therefore, it is possible that early increase of CAV-1 expression was not observed in this study. In such a case, later decrease of eNOS expression can occur, as demonstrated in this study. It is also possible that only higher levels of CAV-1 inhibit eNOS expression and activity [47,48].

We measured nitrite concentration in the media by the Griess reaction, which is the most frequently used method to measure nitrite and is based on spectrophotometric analysis of azo dye obtained after reaction with the Griess reagent. However, this method has some limitations regarding detection limit and sensitivity [49]. Thus, minor changes in nitrite concentration may be not significant despite decreased eNOS activity. Regardless of these limitations, our data suggest that MS preferentially increases paracellular outflow accompanied by weaker interaction between CAV-1 and eNOS.

As MS is known to increase permeability through ROS in both transcellular and paracellular pathways [8,9,15], we hypothesized that MS has an effect on ROS production in the TM. As a result, MS increased generation of ROS, in agreement with previous studies. Thus, MS-induced permeability increase is possibly mediated by the ROS signaling pathway in the TM. Moreover, MS-induced permeability increase was significantly attenuated in the presence of specific ROS inhibitors, further suggesting that ROS are a class of important signaling molecules involved in MS-induced permeability increase. We should consider that MS-induced permeability increase may occur through oth-

er signaling pathways as well; therefore, other related mechanisms should be further investigated.

In conclusion, MS increased permeability across the TM cell monolayer via the paracellular pathway by downregulating the TJ proteins occludin and claudin-5. This MS-induced permeability increase may be mediated through generation of ROS.

Conflict of Interest

No potential conflict of interest relevant to this article was reported.

References

1. Alvarado J, Murphy C, Juster R. Trabecular meshwork cellularity in primary open-angle glaucoma and nonglaucomatous normals. *Ophthalmology* 1984;91:564-79.

2. Rohen JW, Lutjen-Drecoll E, Flugel C, et al. Ultrastructure of the trabecular meshwork in untreated cases of primary open-angle glaucoma (POAG). *Exp Eye Res* 1993;56:683-92.

3. Kopczynski CC, Epstein DL. Emerging trabecular outflow drugs. *J Ocul Pharmacol Ther* 2014;30:85-7.

4. Ashcroft FM, Gribble FM. New windows on the mechanism of action of K(ATP) channel openers. *Trends Pharmacol Sci* 2000;21:439-45.

5. Sica DA. Minoxidil: an underused vasodilator for resistant or severe hypertension. *J Clin Hypertens (Greenwich)* 2004;6:283-7.

6. Nathanson JA. Nitrovasodilators as a new class of ocular hypotensive agents. *J Pharmacol Exp Ther* 1992;260:956-65.

7. Ningaraj NS, Rao MK, Black KL. Adenosine 5'-triphosphate-sensitive potassium channel-mediated blood-brain tumor barrier permeability increase in a rat brain tumor model. *Cancer Res* 2003;63:8899-911.

8. Gu YT, Xue YX, Wang YF, et al. Role of ROS/RhoA/PI3K/PKB signaling in NS1619-mediated blood-tumor barrier permeability increase. *J Mol Neurosci* 2012;48:302-12.

9. Gu YT, Xue YX, Wang YF, et al. Minoxidil sulfate induced the increase in blood-brain tumor barrier permeability through ROS/RhoA/PI3K/PKB signaling pathway. *Neuropharmacology* 2013;75:407-15.

10. Komarova Y, Malik AB. Regulation of endothelial permeability via paracellular and transcellular transport pathways. *Annu Rev Physiol* 2010;72:463-93.

11. Wolburg H, Lippoldt A. Tight junctions of the blood-brain barrier: development, composition and regulation. *Vascul Pharmacol* 2002;38:323-37.

12. Quest AF, Gutierrez-Pajares JL, Torres VA. Caveolin-1: an ambiguous partner in cell signalling and cancer. *J Cell Mol Med* 2008;12:1130-50.

13. Sun SW, Zu XY, Tuo QH, et al. Caveolae and caveolin-1 mediate endocytosis and transcytosis of oxidized low density lipoprotein in endothelial cells. *Acta Pharmacol Sin* 2010;31:1336-42.

14. Surgucheva I, Surguchov A. Expression of caveolin in trabecular meshwork cells and its possible implication in pathogenesis of primary open angle glaucoma. *Mol Vis* 2011;17:2878-88.

15. Gu YT, Xue YX, Zhang H, et al. Adenosine 5'-triphosphate-sensitive potassium channel activator induces the up-regulation of caveolin-1 expression in a rat brain tumor model. *Cell Mol Neurobiol* 2011;31:629-34.

16. Nag S, Venugopalan R, Stewart DJ. Increased caveolin-1 expression precedes decreased expression of occludin and claudin-5 during blood-brain barrier breakdown. *Acta Neuropathol* 2007;114:459-69.

17. Stamer WD, Clark AF. The many faces of the trabecular meshwork cell. *Exp Eye Res* 2017;158:112-23.

18. Gipson IK, Anderson RA. Actin filaments in cells of human trabecular meshwork and Schlemm's canal. *Invest Ophthalmol Vis Sci* 1979;18:547-61.

19. Lepple-Wienhues A, Rauch R, Clark AF, et al. Electrophysiological properties of cultured human trabecular meshwork cells. *Exp Eye Res* 1994;59:305-11.

20. Wiederholt M, Bielka S, Schweig F, et al. Regulation of outflow rate and resistance in the perfused anterior segment of the bovine eye. *Exp Eye Res* 1995;61:223-34.

21. Wiederholt M, Thieme H, Stumpff F. The regulation of trabecular meshwork and ciliary muscle contractility. *Prog Retin Eye Res* 2000;19:271-95.

22. Mosmann T. Rapid colorimetric assay for cellular growth and survival: application to proliferation and cytotoxicity assays. *J Immunol Methods* 1983;65:55-63.

23. Freimoser FM, Jakob CA, Aebi M, Tuor U. The MTT [3-(4,5-dimethylthiazol-2-yl)-2,5-diphenyltetrazolium bromide] assay is a fast and reliable method for colorimetric determination of fungal cell densities. *Appl Environ Microbiol* 1999;65:3727-9.

24. Araie M. Carboxyfluorescein. A dye for evaluating the corneal endothelial barrier function in vivo. *Exp Eye Res* 1986;42:141-50.

25. Grimes PA. Carboxyfluorescein transfer across the blood-retinal barrier evaluated by quantitative fluorescence microscopy: comparison with fluorescein. *Exp Eye Res* 1988;46:769-83.

26. Nakagawa S, Usui T, Yokoo S, et al. Toxicity evaluation of antiglaucoma drugs using stratified human cultivated corneal epithelial sheets. *Invest Ophthalmol Vis Sci* 2012;53:5154-60.

27. Lei Y, Stamer WD, Wu J, Sun X. Oxidative stress impact on barrier function of porcine angular aqueous plexus cell monolayers. *Invest Ophthalmol Vis Sci* 2013;54:4827-35.

28. Srinivasan B, Kolli AR, Esch MB, et al. TEER measurement techniques for in vitro barrier model systems. *J Lab Autom* 2015;20:107-26.

29. Wilhelm I, Fazakas C, Krizbai IA. In vitro models of the blood-brain barrier. *Acta Neurobiol Exp (Wars)* 2011;71:113-28.

30. Green LC, Wagner DA, Glogowski J, et al, Tannenbaum SR. Analysis of nitrate, nitrite, and [15N]nitrate in biological fluids. *Anal Biochem* 1982;126:131-8.

31. Ammar DA, Hamweyah KM, Kahook MY. Antioxidants protect trabecular meshwork cells from hydrogen peroxide-induced cell death. *Transl Vis Sci Technol* 2012;1:4

32. Wang H, Joseph JA. Quantifying cellular oxidative stress by dichlorofluorescein assay using microplate reader. *Free Radic Biol Med* 1999;27:612-6.

33. Alvarado JA, Wood I, Polansky JR. Human trabecular cells. II. Growth pattern and ultrastructural characteristics. *Invest Ophthalmol Vis Sci* 1982;23:464-78.

34. Salama NN, Eddington ND, Fasano A. Tight junction modulation and its relationship to drug delivery. *Adv Drug Deliv Rev* 2006;58:15-28.

35. Grierson I, Lee WR. Pressure-induced changes in the ultrastructure of the endothelium lining Schlemm's canal. *Am J Ophthalmol* 1975;80:863-84.

36. Epstein DL, Rohen JW. Morphology of the trabecular meshwork and inner-wall endothelium after cationized ferritin perfusion in the monkey eye. *Invest Ophthalmol Vis Sci* 1991;32:160-71.

37. Raviola G, Raviola E. Paracellular route of aqueous outflow in the trabecular meshwork and canal of Schlemm. A freeze-fracture study of the endothelial junctions in the sclerocorneal angel of the macaque monkey eye. *Invest Ophthalmol Vis Sci* 1981;21:52-72.

38. Ethier CR. The inner wall of Schlemm's canal. *Exp Eye Res* 2002;74:161-72.

39. Tripathi RC. Mechanism of the aqueous outflow across the trabecular wall of Schlemm's canal. *Exp Eye Res* 1971;11:116-21.

40. Tarkkanen A, Niemi M. Enzyme histochemistry of the angle of the anterior chamber of the human eye. *Acta Ophthalmol (Copenh)* 1967;45:93-9.

41. Michel JB, Feron O, Sacks D, Michel T. Reciprocal regulation of endothelial nitric-oxide synthase by Ca2+-calmodulin and caveolin. *J Biol Chem* 1997;272:15583-6.

42. Ju H, Zou R, Venema VJ, Venema RC. Direct interaction of endothelial nitric-oxide synthase and caveolin-1 inhibits synthase activity. *J Biol Chem* 1997;272:18522-5.

43. Schubert W, Frank PG, Woodman SE, et al. Microvascular hyperpermeability in caveolin-1 (-/-) knock-out mice. Treatment with a specific nitric-oxide synthase inhibitor, L-NAME, restores normal microvascular permeability in Cav-1 null mice. *J Biol Chem* 2002;277:40091-8.

44. Lei Y, Song M, Wu J, et al. eNOS activity in CAV1 knock-out mouse eyes. *Invest Ophthalmol Vis Sci* 2016;57:2805-13.

45. Yu J, Bergaya S, Murata T, et al. Direct evidence for the role of caveolin-1 and caveolae in mechanotransduction and remodeling of blood vessels. *J Clin Invest* 2006;116:1284-91.

46. Parton RG, Simons K. The multiple faces of caveolae. *Nat Rev Mol Cell Biol* 2007;8:185-94.

47. Garcia-Cardena G, Martasek P, Masters BS, et al. Dissecting the interaction between nitric oxide synthase (NOS) and caveolin. Functional significance of the nos caveolin binding domain in vivo. *J Biol Chem* 1997;272:25437-40.

48. Chen Z, D S Oliveira S, Zimnicka AM, et al. Reciprocal regulation of eNOS and caveolin-1 functions in endothelial cells. *Mol Biol Cell* 2018;29:1190-202.

49. Giustarini D, Dalle-Donne I, Colombo R, et al. Adaptation of the Griess reaction for detection of nitrite in human plasma. *Free Radic Res* 2004;38:1235-40.